

## Stabilized laser system at 1550 nm wavelength for future gravitational-wave detectors

Fabian Meylahn<sup>✉</sup>,\* Nicole Knust<sup>✉</sup>, and Benno Willke<sup>✉</sup>

*Max-Planck-Institut für Gravitationsphysik (Albert-Einstein-Institut) and Leibniz Universität Hannover, Callinstraße 38, 30167 Hannover, Germany*

 (Received 3 March 2022; accepted 26 May 2022; published 22 June 2022)

Proposed future gravitational wave detectors place high demands on their prestabilized laser system. We present a prototype for such a prestabilized laser system at 1550 nm wavelength with frequency and power stabilizations optimized for the needs of gravitational wave detectors. A power stabilization with shot noise limited operation below a relative power noise of  $1 \times 10^{-8} \text{ Hz}^{-1/2}$  between 100 Hz to 100 kHz and an active frequency stabilization with a unity-gain bandwidth above 2 MHz were operated simultaneously. Out-of-loop measurements are performed to characterize the achieved stability and to analyze sensor noise limits. We find that nonlinear noise couplings at the spatial mode-filter cavity are of high relevance and lead to increased frequency stability requirements above 100 kHz. This prestabilized laser system can serve as the baseline for the Einstein Telescope gravitational wave detector [ET steering committee, Design report Update 2020 for the Einstein Telescope, Technical Report, Einstein gravitational wave Telescope, 2020.] and demonstrates stabilization concepts generally applicable to optical precision experiments.

DOI: [10.1103/PhysRevD.105.122004](https://doi.org/10.1103/PhysRevD.105.122004)

### I. INTRODUCTION

The detection of gravitational waves in recent years opens a new way of looking at the Universe by detecting signals of inspiraling black holes and neutron stars [1,2]. These detections were made with the second generation of km-scale interferometric gravitational wave detectors (GWDs) that are constantly being improved [3–5].

A third generation of GWDs is currently under development, with the goal of significantly improved sensitivities accompanied by more stringent requirements for all detector subsystems [6,7].

Besides quantum noise, the sensitivity will be mainly limited by the thermal noise of the mirror coatings [8,9]. Therefore, some of the proposed GWDs will be operated with cryogenic cooled silicon mirrors to lower the coating Brownian thermal noise [6,7] compared to current room temperature detectors [3,4,10].

The use of silicon mirrors requires a change to a longer wavelength like  $1.5 \mu\text{m}$  or to about  $2 \mu\text{m}$ , as silicon is not transparent at the currently used wavelength of 1064 nm. Therefore, reliable single-mode, single-frequency lasers at

these wavelengths are required and need to be stabilized to the above-mentioned low noise levels by means of sophisticated methods.

The required output power of the laser system depends on the interferometer configuration and on the desired sensitivity. In the case of the European Einstein Telescope GWD project a laser power of about 3 W is needed to achieve the design sensitivity of its low-frequency interferometers [7].

To reach the needed noise performance of the laser, active feedback stabilizations for the laser power and frequency are necessary. These stabilizations are typically cascaded into a prestabilization of the laser system with sensors close to the laser and the final stabilization with sensors in the main vacuum system of the GWD [11]. In addition to active feedback control, GWDs typically use passive noise reduction techniques via optical cavities, so called mode cleaners.

In this paper we report on the design and operation of a prestabilized laser system (PSL) at 1550 nm wavelength. We identified a master-oscillator power amplifier (MOPA) arrangement with a pre-mode-cleaner (PMC) cleaner as the optimal arrangement for highly reliable operation and high speed control capabilities to operate the necessary frequency and power stabilizations.

We characterize the noise suppression of the stabilization control loops via in-loop sensors and by measurements with independent out-of-loop sensors. Based on the stability achieved, the demonstrated laser system can be considered to be a promising candidate for the Einstein Telescope GWD [7].

\*fabian.meylahn@aei.mpg.de

*Published by the American Physical Society under the terms of the Creative Commons Attribution 4.0 International license. Further distribution of this work must maintain attribution to the author(s) and the published article's title, journal citation, and DOI. Open access publication funded by the Max Planck Society.*

## II. EXPERIMENTAL SETUP

After a detailed characterization of several commercially available single-frequency laser sources at 1550 nm wavelength and several amplifiers [12] we chose a specific MOPA combination with the best performance parameters for a GWD PSL. The selection criteria were a low free-running frequency and power noise in the Fourier frequency range from 1 Hz to 10 MHz as well as suitable power and frequency actuators for high performance feedback stabilizations.

The seed laser is an external cavity diode laser (ECDL) (Orion grade 5) [13] with a waveguide Bragg grating for distributed feedback. It was chosen for its low power noise and fast frequency tunability. The output power of the seed laser is about 10 mW. This seed laser is amplified in a first step to 40 mW by a fiber coupled semiconductor quantum well amplifier (BOA1004P) [14]. With a self-developed power supply, based on [15,16], the amplifier preserves the noise performance of the seed laser and adds a high-speed power modulation option to the laser system.

For final power amplification, an erbium based fiber amplifier (Boostik) [17] is integrated into the PSL. We have tested a 2 W and a 10 W version of this amplifier with similar free-running noise performance. For practical reasons we used the 2 W version for the full PSL demonstration described below [18]. The Boostik fiber amplifier was chosen in our MOPA arrangement as it allows a

modular connection of a seed laser and due to its observed reliability in long-term operation.

The all-fiber MOPA laser system is integrated into a free-space PSL setup including out-of-loop sensors as sketched in Fig. 1.

A fraction of the laser light is analyzed with an in-house build automated laser analysis tool, called diagnostic breadboard (DBB). The free-running power, frequency, and pointing noise of the laser can be analyzed as well as the laser beam's spatial mode composition [19].

The main laser beam is coupled to a PMC, which is a bow-tie style traveling wave optical resonator. The free spectral range of the cavity is 207 MHz and the finesse of 514 is calculated from the pole frequency of 201 kHz, measured via an amplitude modulation transfer function [20]. A flat mirror with 99.4% reflectivity is the in-coupling mirror to this rigid-spacer cavity and a similar mirror is used for the out coupling of the main beam. The bow-tie cavity is close to the impedance matched state as only a small fraction of the circulating light leaves the cavity through the curved mirrors for power stabilization and out-of-loop power noise sensing purposes. The length of the PMC is stabilized to resonate the laser light using a piezoelectric transducer (PZT) placed between the cavity spacer and one of the curved cavity mirrors. The error signal for the length stabilization is generated using the Pound-Drever-Hall (PDH) technique [21,22] and is sent via

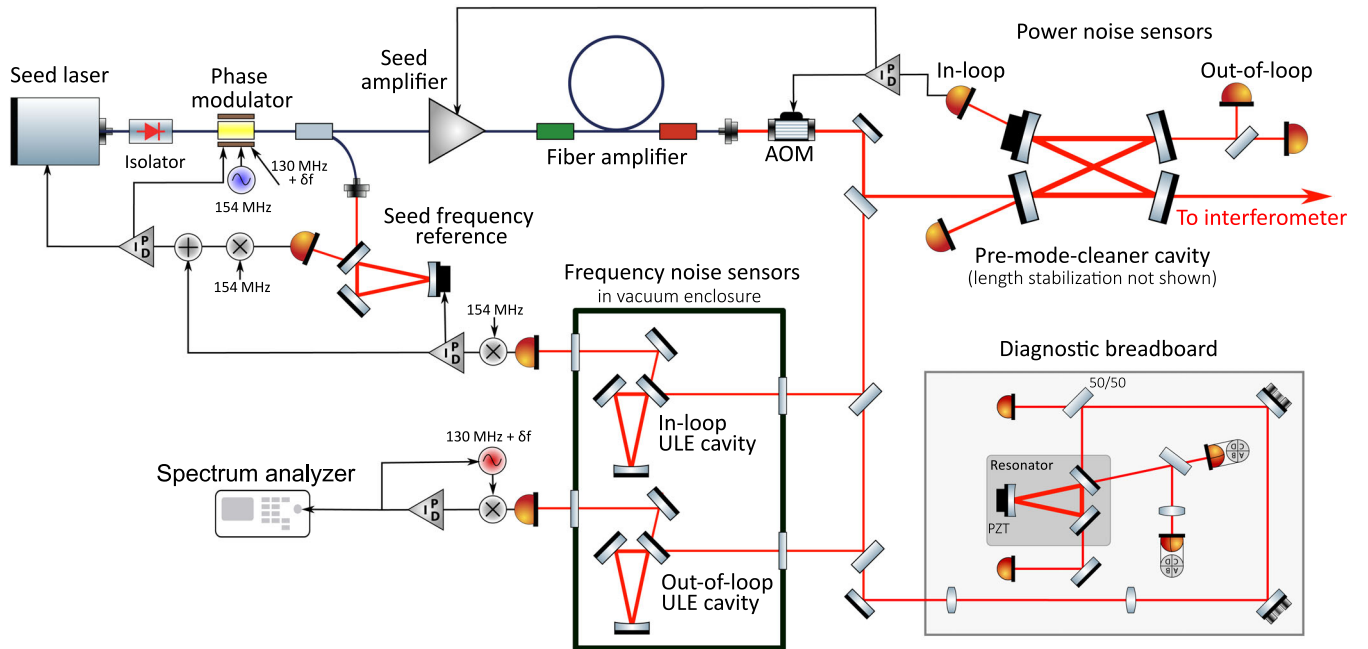


FIG. 1. The schematic setup of the prestabilized laser system shows the seed laser with two laser amplifiers (upper left) and the pre-mode-cleaner cavity (PMC) that transmits the main beam for the GWD interferometer (upper right). One low-power beam for power stabilization and two low-power beams for out-of-loop sensing are shown as well. The seed frequency reference and in-vacuum ultra low expansion glass ceramic cavities used as the main frequency references for in-loop and out-of-loop sensing are shown at the lower left. A diagnostic breadboard for automated free-running laser noise measurements is depicted at the lower right of the sketch.

an analog controller to the above mentioned PZT for actuation of the cavity length.

### A. Seed frequency stabilization

It was found that the power noise of the laser beam transmitted through the stabilized PMC cavity is increased compared to the noise of the injected beam (see Fig. 2). Simulations indicate that this effect is caused by nonlinear down-conversion of frequency noise of the laser between 100 kHz and a few MHz. The nonlinearity is caused by the quadratic dependence of the transmitted laser power on a small frequency mismatch between laser frequency and cavity resonance frequency.

To reduce this excess noise a particularly fast seed laser frequency stabilization (inner loop) is implemented into the setup. A small fraction of the seed laser light is picked off with a fiber coupler after a fiber Faraday isolator and a fiber phase modulator and is sent to a breadboard with a triangular, length tunable rigid-spacer cavity. For the stabilization of the laser frequency the PDH technique is used and the feedback signals are sent to the laser's frequency actuator and above 10 kHz to the phase modulator (see Fig. 1). We achieved a unity-gain frequency (UGF) of 2.1 MHz for this feedback control loop. In comparison to current GWDs, this inner loop frequency stabilization is a factor of  $>6$  faster [11,23]. No particular care was taken to isolate the seed frequency reference from environmental disturbances as the main frequency stabilization of the PSL in GWDs is performed with so-called outer loops that stabilize the laser with respect to well-isolated frequency references. Such references are provided as integral parts of the GWD's optical layout, e.g., input

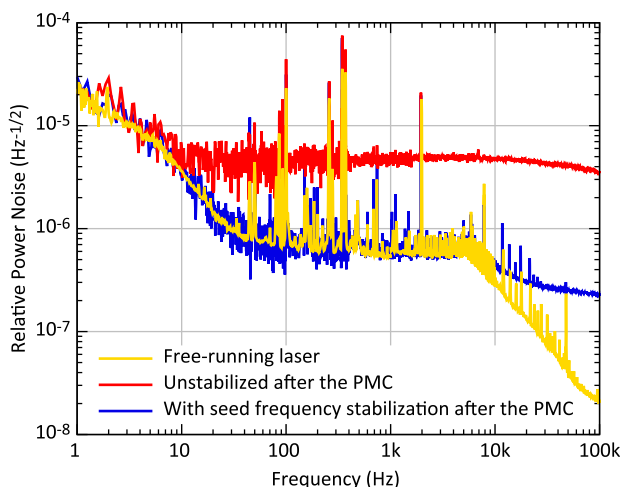


FIG. 2. The power noise of the free-running laser (yellow curve) is lower than the power noise in transmission of the PMC (red curve). This is due to nonlinear frequency-noise to power-noise coupling in the PMC that can be lowered by a fast frequency stabilization of the seed laser (blue curve). (All measurements were taken with disabled power stabilization.)

mode cleaners, power recycling or arm cavities. The high UGF of the inner loop frequency stabilization allows for the implementation of high noise suppression for the outer feedback control loops.

In our experiment we use isolated ultra-low expansion glass ceramic (ULE) cavities to represent such frequency references (see next paragraph). The main purpose of the seed frequency stabilization is to suppress the fast frequency fluctuations of the laser that lead to the increased power noise in transmission of the PMC. The achieved noise reduction can be seen in Fig. 2.

### B. Frequency stabilization to an isolated reference cavity

For the demonstration of a laser frequency stabilization, two almost identical stable triangular cavities with rigid ULE spacers are used. All mirrors of the in-loop cavity and the planar mirrors of the out-of-loop cavity are optically contacted to the spacer. The curved mirror of the out-of-loop cavity is glued. The cavities are placed on fluorine rubber pads inside a vacuum tank with a pressure of  $2 \times 10^{-2}$  mbar for acoustic and seismic shielding. A power of 18.6 mW is injected into the in-loop reference cavity and a power of 6.5 mW is used for the out-of-loop frequency noise measurements.

The free spectral range of the ULE cavities is 702 MHz and the measured pole frequencies are 115 kHz for the in-loop cavity and 132 kHz for the out-of-loop cavity.

The laser frequency is stabilized with a UGF of 180 kHz to the resonance of the in-loop ULE cavity. The error signal is generated with the PDH technique and the feedback is split into two paths. The low frequency tuning is performed by acting on the length of the seed frequency reference and for high frequencies, the feedback is added to the error point of the seed frequency stabilization loop.

### C. Out-of-loop frequency noise measurement

An independent analysis of the frequency noise of the stabilized laser is performed using the out-of-loop ULE cavity. Because of a small length difference of the two rigid ULE cavities, they are not resonant at exactly the same laser frequency. In our case the resonance frequencies are about 130 MHz apart with a small dependence on the mounting of the cavities and the lab temperature.

We imprinted additional phase modulation side bands onto the laser at exactly the difference frequency between the two cavity resonance frequencies, using the fiber phase modulator. Via demodulation of the photodiode signal in reflection of the out-of-loop cavity with this modulation frequency we could generate an error signal that is proportional to the frequency difference between one phase modulation sideband and the out-of-loop cavity's resonance frequency. For a constant modulation frequency, the sideband's frequency fluctuations are identical to the frequency fluctuations of the carrier. Hence, the generated

error signal carries information of the carrier frequency fluctuations with respect to the out-of-loop's frequency reference.

A feedback control loop with 25 kHz UGF is used to control the phase modulation frequency, such that the phase modulation sideband is kept resonant in the out-of-loop ULE cavity. This ensures that the error signal is always valid and has a constant slope, independent of slow drifts between the in-loop and out-of-loop cavities. By capturing the error and control signal of that feedback loop, the out-of-loop measurement of the frequency noise is performed.

#### D. Power stabilization

The sensor for the power stabilization of the laser system is placed in one of the low-power transmission ports of the PMC. This is beneficial, as the power noise added by the PMC via frequency-noise to power-noise conversion and beam pointing to power-noise conversion can be sensed together with the original laser power noise at this port. The power noise from these different origins can simultaneously be suppressed with a single control loop. The light that leaves the other low-power port of the PMC is split equally and sent to two out-of-loop photodiodes. The power in the in-loop and out-of-loop ports is detected by InGaAs photodiodes in combination with active transimpedance amplifiers.

Using the in-loop sensor and a voltage reference, a power-noise error signal is generated and a feedback controller acts on the semiconductor amplifier's pump current for noise suppression at high frequencies. Drifts at low frequencies are compensated with an acousto-optical modulator placed in the in-air propagation path of the 2W laser beam. A UGF of 1.1 MHz is achieved. This UGF is a factor of  $>13$  higher than in current GWDs [3,24], which is beneficial for the noise suppression and for the implementation of an outer loop power stabilization.

The two out-of-loop sensors allow for two individual out-of-loop power-noise measurements. They are also used for a cross-spectral measurement, accessing the power noise below the shot noise limit of the out-of-loop detectors [25].

### III. RESULTS AND DISCUSSION

The free-running laser noise of the MOPA laser system was monitored with the diagnostic breadboard [19]. Every 6 hours a set of measurements was taken. Forty seven measurements of the free-running power noise over an exemplary time period of 12 days are shown in Fig. 3. The deviation between the measurements are very small, such that the shown 47 traces mainly lie on top of each other. The frequency independent noise floor between 5 Hz and 10 kHz is caused by the fiber amplifier. A similar noise signature was measured in all tested erbium based fiber

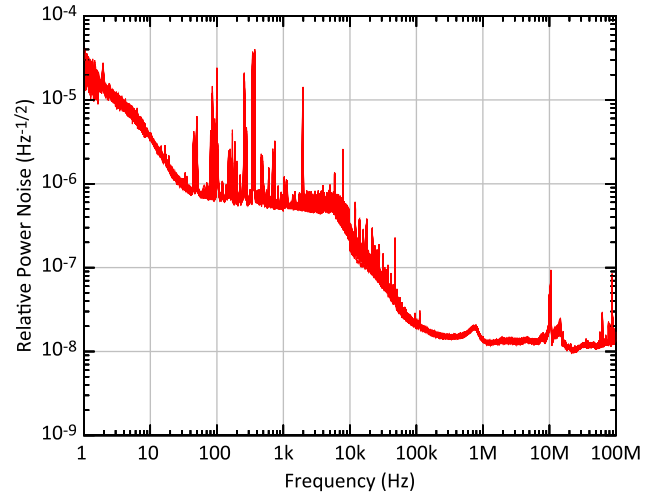


FIG. 3. Free-running relative power-noise measurements of the MOPA system (47 independent curves). The measurements are taken over a time period of 12 days with the automated diagnostic breadboard.

amplifiers and is shaped by the pump light to the output-power transfer function of the amplifier [12].

The data from the 47 frequency noise measurements are shown in Fig. 4. This noise shows the typical shape of the noise of an ECDL, namely, a  $1/f$  noise at low frequencies and above 10 kHz, an almost frequency independent noise [26]. In the full frequency band, the seed laser dominates the measured frequency noise of the MOPA system [12]. These measurements demonstrate the stationarity of the free-running laser noise of the chosen MOPA configuration.

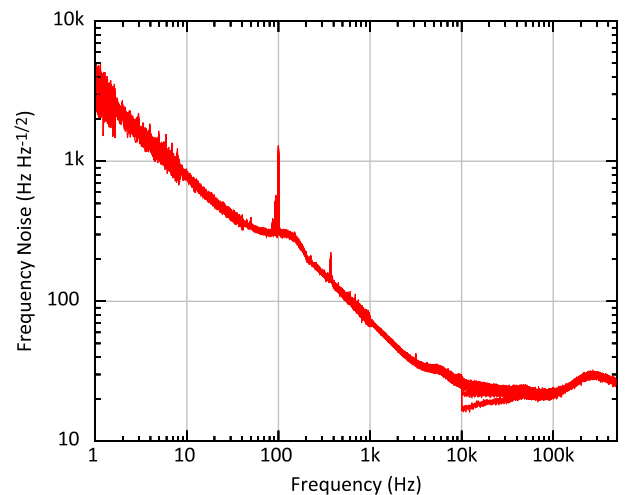


FIG. 4. Free-running frequency-noise measurements of the MOPA system (47 independent curves). The measurements are taken over a time period of 12 days. Each curve is compiled from the error and control signal of a length stabilized cavity in the diagnostic breadboard. Above 10 kHz a different readout electronic was used, which show in a few traces measurement artifacts.

### A. Frequency stabilizations

To measure the frequency noise of the stabilized laser, three optical cavities, which are not part of the frequency stabilization loops, are available in our setup. The resonator in the DBB, with a 31 mm PZT for length tuning, is designed to measure the frequency noise of the free-running lasers. Because of the length noise of its long PZT, this sensor is not sensitive enough to analyze a frequency stabilized laser. Furthermore, the implemented dither modulation technique limits the highest measurement frequency to a Fourier frequency of 500 kHz. The length stabilization of the PMC uses the PDH technique to generate the error signal. Thereby, frequency noise measurements to higher Fourier frequencies are possible. However, this cavity is similar to the DBB cavity sensitive to low frequency acoustic noise coupling and via the installed PZT length actuator sensitive to electronic noise. As both effects limit the low frequency performance of the DBB and PMC, we use a second ULE cavity inside the vacuum system for out-of-loop frequency noise measurement at lower frequencies.

The frequency stabilization follows a nested control loop design. The inner loop frequency stabilization reduces seed laser frequency fluctuations with respect to a triangular cavity. As described above, the main purpose of this control loop is to lower the frequency noise at high Fourier frequencies. Therefore, the stabilization loop is designed with the very high UGF of 2.1 MHz but also with a gain margin of 6 dB and a phase margin of  $63^\circ$  to ensure robust operation with only small excess noise around the UGF.

This can be seen in Fig. 5, which shows the frequency noise of the light that leaves the PMC in the direction of a potential GWD interferometer. Measurements in different states of the inner and outer frequency control loops as measured with the PMC are projected to the light transmitted by the PMC. Here we take the PMC as a frequency reference and calculate the frequency noise from the error signal of the PMC control loop. The yellow curve shows the free-running noise of the MOPA system and the noise reduction in the red curve results from engaging the inner frequency stabilization loop. The effect of the passive noise filter function of the PMC can be seen above its pole frequency of 201 kHz in the yellow curve in comparison to the dashed measurement with the DBB in Fig. 5. As expected, the high gain and phase margins of the inner frequency stabilization avoids any significant increase of the frequency noise above the UGF (Fig. 5, red curve). The frequency noise reduction below 1 MHz strongly reduces the nonlinearly imprinted power noise in transmission of the PMC (see Fig. 2).

The outer loop of the frequency stabilization further reduces the frequency noise of the laser system below 100 kHz, shown in Fig. 5, blue curve. But this feedback control loop has lower phase and gain margins, leading to a small increase in frequency noise above its UGF compared

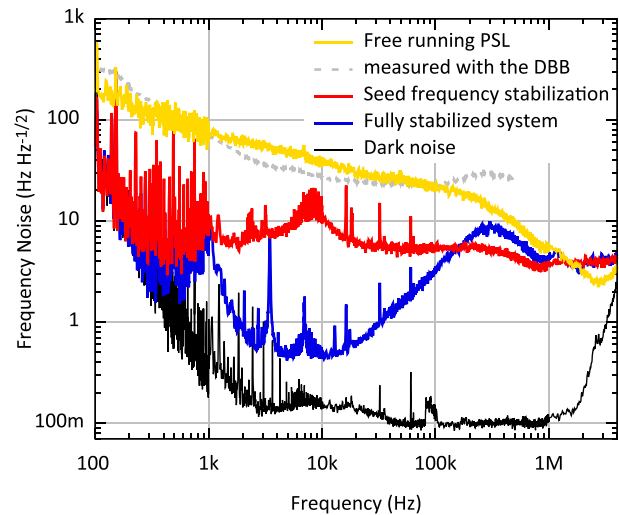


FIG. 5. Frequency noise measurements performed with the PMC. The frequency noise of the free-running laser (yellow curve) is lowered by the seed frequency stabilization (red curve) and is further suppressed by the stabilization to an in-vacuum ULE cavity (blue curve). For comparison, the measurement with the free-running laser is shown (dashed curve). Above 200 kHz the PMC passively filter the frequency noise (compare the dashed to the yellow curve).

to the noise when only the seed stabilization is operating. At low frequencies, dark noise and PMC length noise contaminate the frequency noise measurements.

Another out-of-loop frequency noise measurement is performed with a second ULE cavity inside the vacuum system. As described above, a phase modulation sideband was stabilized to this ULE cavity with a UGF of 25 kHz and the error and control signal of the utilized feedback control loop revealed the frequency noise of the stabilized laser. Figure 6 shows the frequency noise measured with the out-of-loop ULE cavity. It should be noted that the frequency noise is projected to the frequency noise of the light leaving the PMC for a better comparison with Fig. 5. This projection accounts for the line width difference between this ULE cavity and the PMC. With coherence measurements between the control signal of the sideband stabilization loop and a vertical geophone on top of the vacuum tank (L-22D [27]), we confirmed that the noise at frequencies below 1 kHz is correlated to vibrations of the vacuum tank. At frequencies above 10 kHz the achieved noise suppression is limited by the loop gain of the laser frequency stabilization.

### B. Power stabilization

For the active feedback stabilization of the laser power a photodetector at one of the low-power transmission ports of the PMC detects 13 mA photo current. This sensor is used by an analog feedback control loop for a high noise suppression below 100 kHz Fourier frequency.

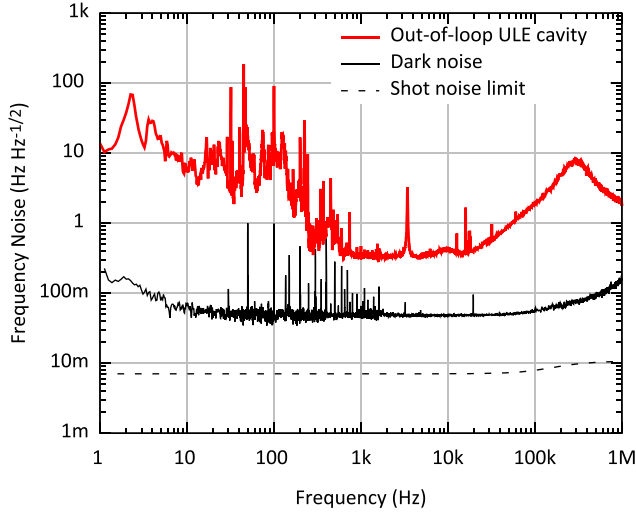


FIG. 6. The out-of-loop frequency noise of the PSL is measured with a second rigid ULE cavity placed in vacuum. From the control and error signals of the stabilization to that cavity, the frequency noise of the stabilized laser at the PMC output is calculated. The shown dark noise is the dark noise of the error signal, which is the technical noise limit for this measurement.

The other low-power PMC port hosts two similar out-of-loop detectors, optimized for low electronic noise [28]. Photo currents of 7 mA and 8 mA, respectively, are detected. In Fig. 7 the out-of-loop relative power-noise measurement of one of these detectors is shown in blue, which is largely limited by the detection shot noise.

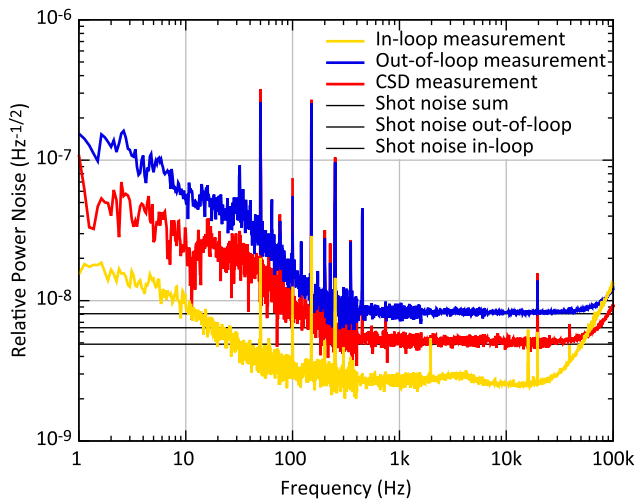


FIG. 7. The out-of-loop relative power noise was measured as an amplitude spectral density with a single photodiode detector (blue curve) and via a cross-spectral density (CSD) measurement between two out-of-loop detectors (red curve). These measurements are compared to the in-loop noise of the power stabilization loop (yellow curve). Above 200 Hz the blue curve is limited by the combined shot noise of the in-loop and out-of-loop detectors, whereas the red curve is limited by the shot noise of the in-loop sensor only (see text for details).

This limit can be bypassed with a cross-spectral density measurement of the signals from the two out-of-loop detectors [25]. This method allows for a power-noise detection that is not limited by the shot noise of the out-of-loop detector and hence represents the noise on the light relevant for the GWD. The measurement presented in Fig. 7, red curve, shows that the power stabilization is limited between 200 Hz and 70 kHz by the shot noise of the in-loop detector, which is at  $5 \times 10^{-9} \text{ Hz}^{-1/2}$ .

Above 70 kHz the power stabilization is loop gain limited and cannot reduce the free-running noise to the shot noise of the in-loop detector. At frequencies below 200 Hz the control loop performance might be limited by the electronic noise of the reference voltage. This noise increases towards low frequencies and can explain the rise of the in-loop noise in Fig. 7. Another noise source at low frequencies is laser beam pointing on the photo diodes and particles passing the laser beam path. Even though the power noise at 1 Hz is roughly 1 order of magnitude above the shot noise, it is still lower than the power noise achieved in earlier experiments with in-air sensing (e.g., [11,29]).

We observed a highly reliable, simultaneous operation of the frequency, power, and PMC length stabilizations without relocks for 16.95 h. After that duration, the continuous operation was interrupted by human interaction.

#### IV. CONCLUSION

We demonstrated a stabilized laser system at a wavelength of 1550 nm for future GWDs, built from commercial lasers, low noise sensors, fast actuators, and analog control loops with high UGFs. Because of the observation of nonlinear frequency-noise to power-noise coupling in the PMC, we implemented a nested control loop configuration for the frequency stabilization of the laser, where the inner loop senses and controls the frequency of the seed laser of a MOPA configuration. This loop provides actuation inputs for an outer loop that will use the GWD interferometer as a frequency reference. In our setup, we use an isolated ULE cavity to mimic that reference and to demonstrate a stable outer loop with a high UGF. This allows for a large gain and an associated high noise reduction in GWDs, where suspended cavities are used for the outermost frequency stabilization.

Similarly, the final GWD power stabilization will send actuation signals to the PSL which in turn requires fast PSL internal power stabilization loops, as presented in this paper. In comparison to the laser systems at 1064 nm wavelength used in currently operating second generation GWDs [30,31], the presented PSL shows increased UGFs of the power stabilization loop, made possible by the fast, integrated power actuator of the semiconductor amplifier and fiber based phase actuators.

The noise performance of the power and frequency stabilization was analyzed with out-of-loop sensors. A second in-vacuum ULE cavity in combination with a

sideband locking scheme revealed low frequency noise down to 400 mHz  $\text{Hz}^{-1/2}$  and a cross-correlation based out-of-loop power detection scheme confirms a shot-noise limited relative power noise of  $5 \times 10^{-9} \text{ Hz}^{-1/2}$ . Although further work is needed to identify and eliminate sensor noise at low Fourier frequencies, the PSL presented demonstrates a control loop topology and performance suitable for future GWDs. In case it is required, the output power of the PSL can be increased via the above-mentioned commercial 10W fiber amplifier or a large mode area  $\text{Er}^{3+}:\text{Yb}^{3+}$  fiber amplifier with output-power levels of 100 W [32]. Although we have focused on GWD applications, the demonstrated PSL can also be used for other

high precision metrology experiments and the stabilization concepts can be applied at different wavelengths, e.g., for a MOPA laser system with ECDLs and semiconductor preamplifier for a GWD operating at 2  $\mu\text{m}$  [6,33].

## ACKNOWLEDGMENTS

This work was supported by Deutsche Forschungsgemeinschaft (DFG, German Research Foundation) under Germany's Excellence Strategy EXC-2123 Quantum Frontiers 390837967.

The authors declare no conflicts of interest.

- 
- [1] The LIGO Scientific, the Virgo, and the KAGRA Collaborations, GWTC-3: Compact binary coalescences observed by LIGO and Virgo during the second part of the third observing run, [arXiv:2111.03606](https://arxiv.org/abs/2111.03606).
- [2] B. P. Abbott *et al.* (LIGO Scientific Collaboration and Virgo Collaboration), Multi-messenger observations of a binary neutron star merger, *Astrophys. J.* **848**, L12 (2017).
- [3] A. Buikema *et al.*, Sensitivity and performance of the Advanced LIGO detectors in the third observing run, *Phys. Rev. D* **102**, 062003 (2020).
- [4] F. Acernese *et al.* (Virgo Collaboration), Advanced Virgo: A second-generation interferometric gravitational wave detector, *Classical Quantum Gravity* **32**, 024001 (2015).
- [5] KAGRA Collaboration, KAGRA: 2.5 generation interferometric gravitational wave detector, *Nat. Astron.* **3**, 35 (2019).
- [6] D. Reitze *et al.*, Cosmic explorer: The U.S. contribution to gravitational-wave astronomy beyond LIGO, *Bull. Am. Astron. Soc.* **51**, 035 (2019), <https://baas.aas.org/pub/2020n7i035>.
- [7] ET steering committee, Design report Update 2020 for the Einstein Telescope, Technical Report, Einstein gravitational wave Telescope, Technical Report No. ET-0007B-20 2020, <https://apps.et-gw.eu/tds/ql/?c=15418>.
- [8] S. Gras and M. Evans, Direct measurement of coating thermal noise in optical resonators, *Phys. Rev. D* **98**, 122001 (2018).
- [9] G. M. Harry, A. M. Gretarsson, P. R. Saulson, S. E. Kittelberger, S. D. Penn, W. J. Startin, S. Rowan, M. M. Fejer, D. R. M. Crooks, G. Cagnoli *et al.*, Thermal noise in interferometric gravitational wave detectors due to dielectric optical coatings, *Classical Quantum Gravity* **19**, 897 (2002).
- [10] C. Affeldt *et al.*, Advanced techniques in GEO 600, *Classical Quantum Gravity* **31**, 224002 (2014).
- [11] P. Kwee, C. Bogan, K. Danzmann, M. Frede, H. Kim, P. King, J. Pödl, O. Puncken, R. L. Savage, F. Seifert, P. Wessels, L. Winkelmann, and B. Willke, Stabilized high-power laser system for the gravitational wave detector Advanced LIGO, *Opt. Express* **20**, 10617 (2012).
- [12] F. Meylahn and B. Willke, Stabilized laser systems at 1550 nm wavelength for future gravitational wave detectors, *Instruments* **6**, 15 (2022).
- [13] OptaSense Inc. (2021), <https://rio-lasers.com>.
- [14] Thorlabs Inc. (2021), <https://www.thorlabs.com>.
- [15] C. J. Erickson, M. V. Zijll, G. Doermann, and D. S. Durfee, An ultrahigh stability, low-noise laser current driver with digital control, *Rev. Sci. Instrum.* **79**, 073107 (2008).
- [16] D. L. Troxel, C. J. Erickson, and D. S. Durfee, Note: Updates to an ultra-low noise laser current driver, *Rev. Sci. Instrum.* **82**, 096101 (2011).
- [17] NKT Photonics A/S (2021), <https://www.nktphotonics.com>.
- [18] We chose the 2 W version, because it comes with a standard FC-APC polarization maintaining fiber output that can be extended with patch fibers, connected to a vacuum feed-through or connected to further amplification stages.
- [19] P. Kwee and B. Willke, Automatic laser beam characterization of monolithic Nd:YAG nonplanar ring lasers, *Appl. Opt.* **47**, 6022 (2008).
- [20] M. Rakhmanov, R. Savage, D. Reitze, and D. Tanner, Dynamic resonance of light in Fabry-Perot cavities, *Phys. Lett. A* **305**, 239 (2002).
- [21] R. Drever, J. L. Hall, F. Kowalski, J. Hough, G. Ford, A. Munley, and H. Ward, Laser phase and frequency stabilization using an optical resonator, *Appl. Phys. B* **31**, 97 (1983).
- [22] E. D. Black, An introduction to Pound–Drever–Hall laser frequency stabilization, *Am. J. Phys.* **69**, 79 (2001).
- [23] F. Acernese *et al.*, Control of the laser frequency of the Virgo gravitational wave interferometer with an in-loop relative frequency stability of  $1.0 \times 10^{-21}$  on a 100 ms time scale, in *2009 IEEE International Frequency Control Symposium Joint with the 22nd European Frequency and Time forum* (IEEE, New York, USA, 2009), pp. 760–763, [10.1109/FREQ.2009.5168287](https://doi.org/10.1109/FREQ.2009.5168287).
- [24] F. Cleva, J.-P. Coulon, L. W. Wei, M. Turconi, M. Merzougui, E. Genin, G. Pillant, and F. Kefelian, Laser power stabilization for advanced VIRGO, in *2021 Conference on Lasers and Electro-Optics Europe & European Quantum Electronics*

- Conference (CLEO/Europe-EQEC)* (IEEE, New York, USA, 2021), [10.1109/CLEO/Europe-EQEC52157.2021.9542330](https://doi.org/10.1109/CLEO/Europe-EQEC52157.2021.9542330).
- [25] J. R. Venneberg and B. Willke, Quantum correlation measurement of laser power noise below shot noise, *Opt. Continuum* **1**, 1077 (2022).
- [26] M. A. Tran, D. Huang, and J. E. Bowers, Tutorial on narrow linewidth tunable semiconductor lasers using si/III-v heterogeneous integration, *APL Photonics* **4**, 111101 (2019).
- [27] R. Kirchhoff, C. M. Mow-Lowry, V. B. Adya, G. Bergmann, S. Cooper, M. M. Hanke, P. Koch, S. M. Köhlenbeck, J. Lehmann, P. Oppermann, J. Wöhler, D. S. Wu, H. Lück, and K. A. Strain, Huddle test measurement of a near johnson noise limited geophone, *Rev. Sci. Instrum.* **88**, 115008 (2017).
- [28] F. Meylahn and P. Kwee, Power stabilization photodiode (2020), <https://dcc.ligo.org/LIGO-D2000510/public>.
- [29] F. Thies, N. Bode, P. Oppermann, M. Frede, B. Schulz, and B. Willke, Nd:YVO4 high-power master oscillator power amplifier laser system for second-generation gravitational wave detectors, *Opt. Lett.* **44**, 719 (2019).
- [30] N. Bode, J. Briggs, X. Chen, M. Frede, P. Fritschel, M. Fyffe, E. Gustafson, M. Heintze, P. King, J. Liu, J. Oberling, R. L. Savage, A. Spencer, and B. Willke, Advanced LIGO laser systems for O3 and future observation runs, *Galaxies* **8**, 84 (2020).
- [31] F. Cleva, J.-P. Coulon, and F. Kéfélian, Characterization, Integration and Operation of a 100-W Solid State Amplifier in the Advanced-VIRGO Pre-Stabilized Laser System, in *CLEO Europe 2019* (Munich, Germany, 2019), [10.1109/CLEO-EQEC.2019.8873060](https://doi.org/10.1109/CLEO-EQEC.2019.8873060).
- [32] O. D. Varona, W. Fittkau, P. Booker, T. Theeg, M. Steinke, D. Kracht, J. Neumann, and P. Wessels, Single-frequency fiber amplifier at 1.5  $\mu\text{m}$  with 100 W in the linearly-polarized TEM00 mode for next-generation gravitational wave detectors, *Opt. Express* **25**, 24880 (2017).
- [33] D. P. Kapasi, J. Eichholz, T. McRae, R. L. Ward, B. J. J. Slagmolen, S. Legge, K. S. Hardman, P. A. Altin, and D. E. McClelland, Tunable narrow-linewidth laser at 2  $\mu\text{m}$  wavelength for gravitational wave detector research, *Opt. Express* **28**, 3280 (2020).